DOI 10.5162/17dss2024/7.2

# Neural Network-Driven Image Gamma Calibration: An Innovative Approach for All-Optical Rheometer

*Tianliang Wang[1], Ehsan Fattahi [1] Dominik Geier[1], Thomas Becker[1]*

*[1] Chair of Brewing and Beverage Technology, Technical University of Munich, Weihenstephaner Steig 20, D-85354 Freising, Germany*
*Contact: tianliang.wang@tum.de*

## Introduction

When coherent light is irradiated onto a fluid sample containing particles, the interference between the scattered light paths forms granular speckles [1, 2]. In the field of optical imaging, researchers aim to reduce such speckle patterns. However, in applications such as blood flow measurement [3], surface roughness assessment [4], and optical sensing [5], speckle patterns play an important role because they carry detailed information about the sample's properties. Laser speckle rheology (LSR) uses speckle patterns to measure the viscoelastic properties of fluids [6], addressing the limitations of traditional methods such as shear rheometers, dynamic light scattering (DLS) [7], and diffusing wave spectroscopy (DWS) [8], which require large samples, direct contact, and bulky equipment. For LSR, the speckle pattern is first used to calculate the autocorrelation curve ($g_2(t)$) to derive the mean square displacement (MSD), which is then used to determine the sample's Complex Modulus ($G^*(\omega)$) [9]. Improvements to LSR, such as the use of polarization-sensitive Monte Carlo algorithms, have improved accuracy by correcting for scattering and absorption effects, resulting in more reliable viscoelastic measurements [10]. LSR has found applications in assessing the biomechanical properties of tissues, particularly in oncology [11, 12].

Despite its many advantages, LSR still faces challenges. To obtain an ideal speckle pattern, three conditions must be met: a high-speed camera to prevent motion artifacts, a sufficient ratio of speckle size to pixel size, and a narrow linewidth illumination source to ensure high contrast [9]. These requirements significantly increase the cost and computational requirements, limiting the method's accessibility. Even under these conditions, additional calibration is often required. In this study, to eliminate the multiple scattering, a new method is proposed to calibrate the $g_2(t)$ curve by directly performing Gamma image correction on the speckle pattern. The method optimizes the MSD calculation, reduces the reliance on high-performance computing resources, and enhances the adaptability to individual sample differences. To enable image calibration, a neural network is designed that predicts an optimal Gamma value for enhancing the speckle pattern based on the statistical characteristics of the image.

## Method and Material

*Experimental setup*

The classic LSR experimental setup uses a helium-neon linearly polarized laser with a wavelength of 632.8nm (17mW) as the illumination source (Fig. 1). The polarized and collimated laser beam first passes through a polarizer (P1). A beam splitter then splits the laser beam, and 50% of the laser irradiates the sample after being focused by a lens. The final backscattered light of the sample is collected by a camera with an optical imaging lens. Another polarizer (P2) is placed in front of the lens with a polarization angle perpendicular to P1 to eliminate specular reflections and capture only the backscattered light from the sample.

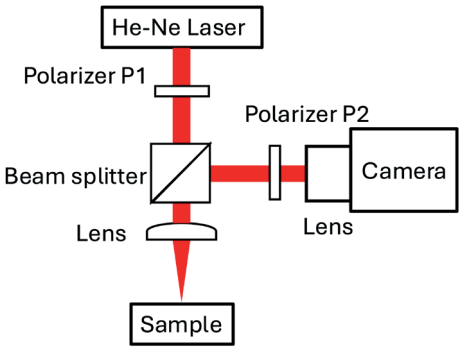


**Fig. 1:** Experimental setup of the LSR system.

*Sample preparation*

The sample for generating the speckle pattern was prepared by mixing glycerol (≥ 99.5% purity, redistilled, analytical grade) with titanium dioxide ($TiO_2$) particles with different volume-to-mass ratios.

*Analysis*

For the LSR method, the core idea is to calculate the intensity fluctuation of the speckle pattern sequence and the dynamic characteristics of the sample. Usually, we use the $g_2(t)$ curve, as shown in Eq. (1), to describe this fluctuation [11].

$$g_2(t) = < \frac{\langle I(t_0) I(t_0+t) \rangle}{\sqrt{\langle I(t_0)^2 \rangle \langle I(t_0+t)^2 \rangle}} > t_0 \quad (1)$$

Where $I(t_0)$ and $I(t_0 + t)$ represent the speckle pattern intensity at the initial time $t_0$ and time $t_0 + t$, respectively. $I(t_0)I(t_0 + t)$ denotes the expected cross-correlation of the speckle pattern intensity at these time points, reflecting the correlation between the intensity at $t_0$ and $t_0 + t$. The denominator represents the expected value of the square of the intensity at each time point, and taking the square root of their product normalizes the correlation function $g_2(t)$. This normalization ensures that the autocorrelation value is 1 at $t = 0$, indicating perfect correlation without any delay. The symbol $t_0$ means the average value taken over all possible initial times $t_0$ to calculate the correlation between the intensities $I(t_0)$ and $I(t_0 + t)$ at different time intervals.

When the particle concentration changes, the decay rate of the $g_2(t)$ curve is seriously affected due to the change in the photon path and coherence. To show this, we plotted the original $g_2(t)$ curves calculated from samples with different particle concentrations of 0.2%, 0.8%, and 2%, as shown in Fig. 2. It can be seen from this figure that when the concentrations increased, the decay speed of the $g_2(t)$ curve increased. The decay of the $g_2(t)$curve is the most critical factor for accurately measuring the $G^*(\omega)$ of the sample. If a suitable intensity correction algorithm can be developed to calibrate without being affected by the concentration, the accuracy of the $G^*(\omega)$ measurement can be significantly improved.

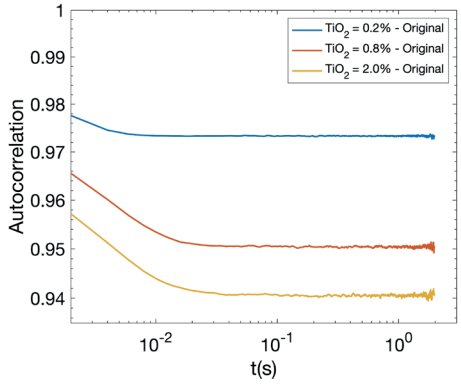


**Fig. 2:** $g_2(t)$ curves of speckle patterns captured from samples with $TiO_2$ concentrations of 0.2%, 0.8%, and 2%.

In addition, we found that image contrast changes when we adjust the concentration of $TiO_2$ particles, as shown in Fig.3. It is calculated as $\sigma(I) / \bar{I}$, where $\sigma(I)$ represents the standard deviation of the speckle pattern and $\bar{I}$ is the average intensity. When the speckle patterns have a higher contrast, usually approximately 1, they are regarded as the well-developed speckle pattern in LSR. In Fig. 3, we can see that when the contraction rises, the contrast of speckle patterns increases simultaneously. This result reveals that the change imposed by the concentration change can be regarded as a function of image intensity. Therefore, we assume that an intensity-related algorithm exists to modulate speckle intensities to eliminate the influences of concentration change.

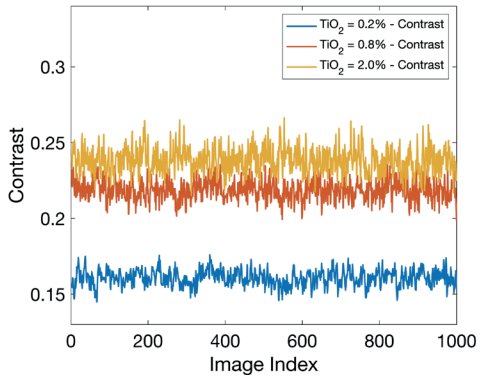


**Fig. 3:** Contrast values of speckle patterns captured from samples with $TiO_2$ concentrations of 0.2%, 0.8%, and 2%.

Taking these factors into account, Gamma correction can be considered the possible way to correct the original speckle pattern. This is because Gamma calibration non-linearly adjusts pixels of different intensities, resulting in a more dispersed intensity distribution and higher contrast [13, 14]. The formula for Gamma correction is shown in Eq.(2),

$$I_{corrected} = \left(\frac{I_{Orginal}}{I_{max}}\right)^{\gamma} \times I_{max} \quad (2)$$

Here, $I_{corrected}$ represents the corrected speckle pattern, $I_{original}$ denotes the uncorrected speckle pattern, $I_{max}$ is the maximum intensity value in the original speckle pattern, and $\gamma$ is the Gamma value. Fig. 4 shows a typical speckle pattern and the corresponding Gamma-corrected one. Once the image is corrected by a Gamma value, its contrast will be increased. In our case, the changed Gamma value can modulate the intensity distribution, making the speckle patterns have higher contrasts (when $\gamma > 1$) and changing the decay speed of the $g_2(t)$ curves.

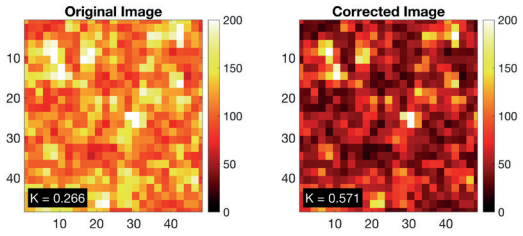


**Fig. 4:** Original speckle patterns and corresponding Gamma-corrected speckle patterns, K is the contrast value.

To evaluate the feasibility of Gamma correction, we set the Gamma value from 1 to 2 with a step size of 0.2 to correct the data set. Subsequently, we applied Eq. (1) to calculate the $g_2(t)$ curves of the original data set and the corrected data set (calibrated by Eq. (2)). The resulting $g_2(t)$ curves are shown in Fig. 5 (a). From these curves, it can be seen that when the Gamma value increases, the $g_2(t)$ curve of the corrected data set decays faster than the original curve.

This indicates that Gamma correction enhances the difference between the intensities at different time points, thereby weakening the temporal correlation. In addition, the contrast values of the corrected speckle patterns, enhanced by different Gamma values, are also shown in Fig. 5 (b). As the Gamma value increases, the contrast gradually increases and approaches higher contrast. The ability to modify the temporal decay by changing the Gamma value highlights the potential of optimizing the speckle pattern to approximate the ideal $g_2(t)$ curve in LSR applications.

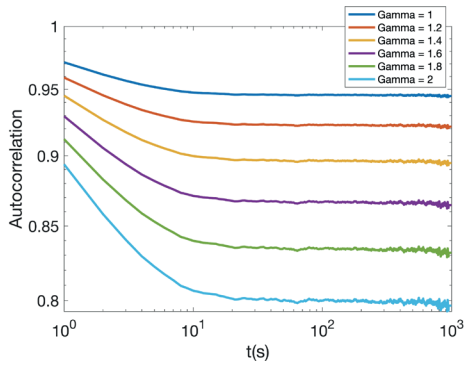


**Fig. 5: (a)** $g_2(t)$ curves of speckle patterns calibrated with different Gamma values

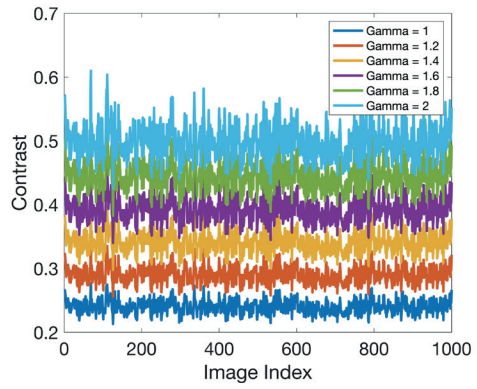


**Fig. 5: (b)** Contrast values of speckle patterns calibrated with different Gamma values

We then use the Gamma-corrected curve to calculate the $G^*(\omega)$ and compare the results with the actual data measured from the shear rheometer. The calculation follows previous work [10], where we introduced the relationship between the $g_2(t)$ curve and the MSD, as shown in Eq. 3 [11]:

$$g_2(\mathrm{t}) = 1 + e^{-2\gamma\sqrt{k_0^2 n^2 \langle \Delta^2(t)\rangle}} \quad (3)$$

Using the corrected $g_2(t)$ curve, we obtain the MSD by curve fitting. In this context, $\gamma$ is the decay constant, $k_0$ represents the wave vector, $n$ is the refractive index of the medium, $\lambda$ is the wavelength of the incident light, and $\langle \Delta r^2(t) \rangle$ represents the mean square displacement (MSD) of the particle, representing its motion over time t. Once the MSD is determined, the $G^*(\omega)$ of the sample can be calculated using the Stokes-Einstein equation:

$$G^*(\omega) = \left. \frac{K_B T}{\pi a \langle \Delta r^2(1/\omega)\rangle \Gamma(1+\alpha(t))} \right|_{\omega=1/t} \quad (4)$$

Where $K_B$ represents the Boltzmann constant ($1.38 \times 10^{-23}$ $J/K$), $T$ represents the absolute temperature in Kelvin, $a$ represents the radius of the scattering particle, $\langle \langle \Delta r^2(t) \rangle \rangle$ represents the MSD at frequency $\omega = 1/t$, $\Gamma$ represents the Gamma function, $\alpha(t) = \partial \log \langle \Delta r^2(t) \rangle / \partial \log t$, and $|\omega = 1/t$ represents the logarithmic slope of the MSD. To show the effect, we used a sample with 100% of Glycerin (denoted as G:W=100:0) and 2% of $TiO_2$ particles. We manually increased the Gamma value to 1.6 and the calibrated $G^*(\omega)$ is shown in Fig. 6. It can be seen that Gamma correction can improve the accuracy of LSR data and bring it closer to the rheometer's reference values.

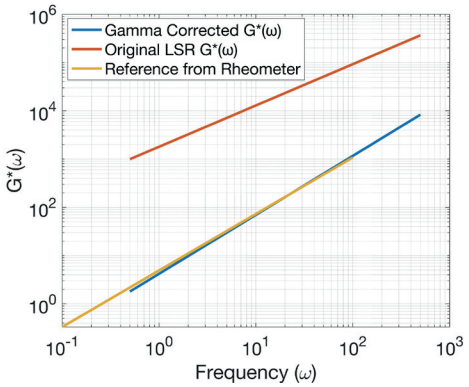


**Fig. 6:** The original and Gamma corrected G*(ω) curves, the Gamma value is 1.6 in this case.

## Results

Since we cannot directly get the optimal Gamma value from the known speckle intensity and $g_2(t)$ curve because the mapping between them is not a linear relationship, we designed a neural network, shown in Fig. 7, to predict the optimal Gamma value. The network has two channels as input: the $g_2(t)$ curve and the contrast of the image sequence. Each data input is processed by the same fully connected layer network (Network 1 and 2 in the figure) to extract features. The output of the network is the predicted optimal Gamma value. The $g_2(t)$ curve and the contrast of the image sequence were used as the input of the network and the output was a neuron.

The $TiO_2$ samples were mixed with solutions with glycerol-water volume ratios of 100:0, 80:20, and 60:40, and the speckle pattern generated by the backscattered light of each sample was recorded.

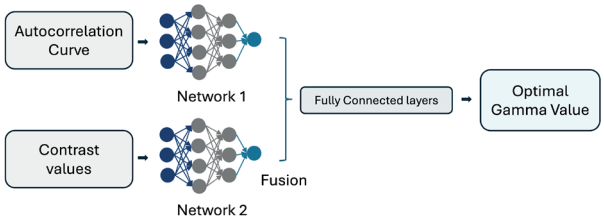


**Fig. 7:** Network structure of the designed network. Networks 1 and 2 have four hidden layers each.

During training, we used mean squared error (MSE) as the loss function [15], the optimizer selected was the Adam optimizer, and the learning rate was set to 0.001. The dataset was shuffled and divided into 60% training, 20% validation, and 20% test sets. The size of each training batch is 32, and the total number of training epochs is 1000. In each epoch iteration, the model performs a complete traversal of the entire training set, including forward propagation to calculate the predicted value, calculate the loss, backpropagation to calculate the gradient, and parameter update. The training and validation loss curves are shown in Fig. 8 (a). As can be seen from the enlarged image, the lowest training and validation losses are 0.00003 and 0.00025, respectively.

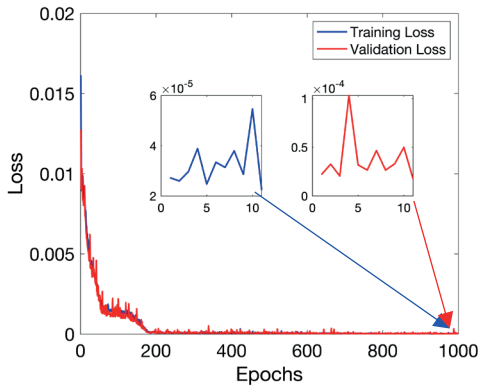


**Fig. 8: (a)** The training and validation loss of the designed network.

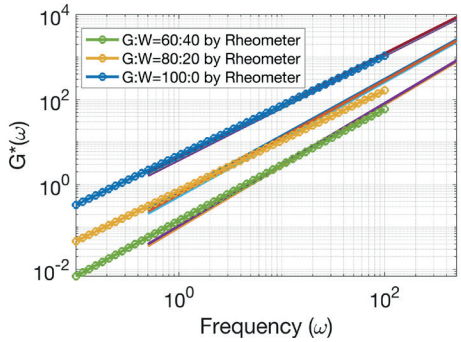


**Fig. 8: (b)** The test results from the predicted Gamma values. The dotted line is the reference curves from the rheometer, while the solid line is the results of curves from samples with different concentrations.

After training, the model is evaluated using the test set, and the predicted Gamma value is applied to enhance the speckle patterns generated by the samples, followed by calculating the final $G^*(\omega)$, see Fig. 8(b).

To validate the accuracy of the previous Gamma correction method, we used other Newtonian samples with different $G^*(\omega)$, condensed milk, and whole milk, acquired new speckle datasets and retrained the network. These samples have different $G^*(\omega)$ and particle (protein and fat) concentrations. Additionally, the experimental conditions were kept consistent with the previous setup. After acquiring the original speckle data, we calculated its $g_2(t)$ curve and contrast values. These values are sent to the retrained network to predict the corresponding Gamma value, which subsequently is used to calibrate the speckle patterns. Finally, we compared the resulting $G^*(\omega)$ curve with the ones measured by the rheometer. The comparison in Fig. 9 showed good consistency between the Gamma-corrected data and the rheometer measurements, confirming that the Gamma correction method is effective across different samples with varying concentrations and $G^*(\omega)$.

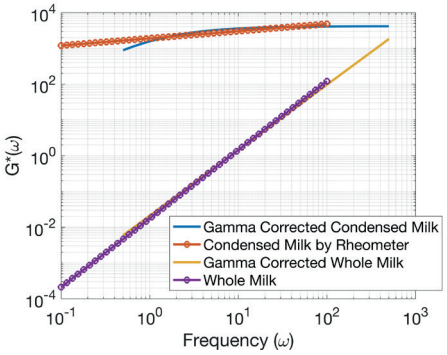


**Fig. 9:** Test results from dairy products

## Discussion and Conclusion

This study successfully demonstrated the effectiveness of neural network-based Gamma calibration in overcoming the multiple scattering problems in LSR systems. Through experiments with different titanium dioxide concentrations, we verified that neural network-based Gamma calibration significantly enhanced the contrast of the speckle image, allowing for a more accurate measurement of the $G^*(\omega)$. Our results suggest that Gamma calibration is a practical and reliable method for speckle pattern analysis in LSR applications. By enhancing image contrast, Gamma calibration can more accurately characterize the $G^*(\omega)$ of complex fluids.

In future research, additional parameters must be addressed. The effectiveness of Gamma calibration depends on carefully adjusting the Gamma value, which may vary depending on experimental conditions and

sample properties. In addition, the impact of environmental noise and other external factors on the calibration process requires further investigation. Future studies will aim to develop automatic algorithms for real-time optimization of Gamma values and explore the applicability of Gamma calibration to other imaging techniques.

In conclusion, Gamma calibration, assisted by neural networks, is a valuable tool for LSR to solve the multiple scattering problem and provides a cost-effective solution for enhanced speckle pattern analysis. Its application can lead to more reliable and accurate measurements, thus deepening our understanding of the viscoelastic properties of complex fluids and making a significant contribution to the field of rheology.

## Acknowledgment

This IGF Project of the FEI (grant number: 01IF22490N) is supported within the programme for promoting the Industrial Collective Research (IGF) of the Federal Ministry of Economic Affairs and Climate Action (BMWK), based on a resolution of the German Parliament

## Reference

[1] Goodman, J.W., Some fundamental properties of speckle. JOSA, 1976. 66(11): p. 1145-1150.
DOI: 10.1364/JOSA.66.001145

[2] Goodman, J.W., Speckle phenomena in optics: theory and applications. 2007: Roberts and Company Publishers.

[3] Briers, J.D., Laser speckle contrast imaging for measuring blood flow. Optica Applicata, 2007. 37.

[4] Dhanasekar, B., et al., Evaluation of surface roughness based on monochromatic speckle correlation using image processing. Precision Engineering, 2008. 32(3): p. 196-206.
DOI: 10.1016/j.precisioneng.2007.08.005

[5] Wang, T., et al., Deep-learning-assisted fiber Bragg grating interrogation by random speckles. Optics Letters, 2021. 46(22): p. 5711-5714.
DOI: 10.1364/OL.445159

[6] Kashany, Z.H. and S. Nadkarni. Laser speckle rheological microscopy reveals the associations between micro-mechanical properties and immune response of the tumor microenvironment. in Optical Elastography and Tissue Biomechanics XI. 2024. SPIE.

[7] Stetefeld, J., S.A. McKenna, and T.R. Patel, Dynamic light scattering: a practical guide and applications in biomedical sciences. Biophysical reviews, 2016. 8: p. 409-427.
DOI: 10.1007/s12551-016-0218-6

[8] Badruddoza, A.Z.M., et al., Diffusing wave spectroscopy (DWS) methods applied to double emulsions. Current opinion in colloid & interface science, 2018. 37: p. 74-87.
DOI: 10.1016/j.cocis.2018.06.006

[9] Hajjarian, Z. and S.K. Nadkarni, Tutorial on laser speckle rheology: technology, applications, and opportunities. Journal of biomedical optics, 2020. 25(5): p. 050801-050801.
DOI: 10.1117/1.JBO.25.5.050801

[10] Hajjarian, Z. and S.K. Nadkarni, Evaluation and correction for optical scattering variations in laser speckle rheology of biological fluids. PloS one, 2013. 8(5): p. e65014.
DOI: 10.1371/journal.pone.0065014

[11] Leartprapun, N., et al., Laser speckle rheological microscopy reveals wideband viscoelastic spectra of biological tissues. Science Advances, 2024. 10(19): p. eadl1586.
DOI: 10.1126/sciadv.adl1586

[12] Zhao, Y., et al., Transmission laser speckle rheological method with measurable viscoelasticity of biological liquid inside tissue. Optics Communications, 2022. 504: p. 127451.
DOI: 10.1016/j.optcom.2021.127451

[13] Rahman, S., et al., An adaptive gamma correction for image enhancement. EURASIP Journal on Image and Video Processing, 2016. 2016: p. 1-13.
DOI: 10.1186/s13640-016-0138-1

[14] Guan, X., et al. An image enhancement method based on gamma correction. in 2009 Second international symposium on computational intelligence and design. 2009. IEEE.

[15] Christoffersen, P. and K. Jacobs, The importance of the loss function in option valuation. Journal of Financial Economics, 2004. 72(2): p. 291-318.
DOI: 10.2139/ssrn.424461